Multi-step two-copy distillation of squeezed states via two photon subtraction

— Supplementary Material —

Stephan Grebien,[1] Julian Göttsch,[1] Boris Hage,[2] Jaromír Fiurášek,[3] and Roman Schnabel[1,*]

[1] *Institut für Laserphysik & Zentrum für Optische Quantentechnologien, Universität Hamburg, Luruper Chaussee 149, 22761 Hamburg, Germany*

[2] *Institut für Physik, Universität Rostock, 18051 Rostock, Germany*

[3] *Department of Optics, Faculty of Science, Palacký University, 17. listopadu 12, 77900 Olomouc, Czech Republic*

(Dated: March 21, 2022)

TEMPORAL MODE FUNCTION OF PHOTON SUBTRACTED STATE

The quantum state from that two photons are subtracted belongs to a Fourier-transform limited mode whose temporal and spectral profiles are defined by the optical setup as well as the properties of the photon counters. We determine the temporal profile $f(t)$ in the course of our ensemble measurement. We used the covariance matrix of the anti-squeezed quadrature $\hat{X}^Q$, following the approach of Ref. [1]. Specifically, we sought a temporal mode that maximised the variance of the anti-squeezed quadrature, because this mode was expected to contain the two-photon subtracted state. Since we sampled the quadrature at 160 discrete times t_m, the resulting covariance matrix C was a finite square matrix with 160 columns and rows,

$$C_{mn} = \langle \Delta \hat{X}^Q(t_m) \Delta \hat{X}^Q(t_n) \rangle.$$

A reference measurement on ensemble of the vacuum state revealed that the covariance matrix of vacuum D was not an identity matrix, and some correlations between nearby quadratures were present. This could be attributed to fast sampling of the quadratures together with finite bandwidth of the detector. The actually measured quadratures $\hat{X}^Q(t_j)$ were then given by the convolution of the input quadratures with temporal response function of the detector.

The variance of the $\hat{X}$ quadrature of temporal mode $f(t)$ can be expressed as

$$\Delta^2 \hat{X}^Q_{\text{mode}} = \frac{f(t)^T C f(t)}{f(t)^T D f(t)}.$$

Here $f(t)$ is treated as a column vector and the variance is properly normalised such that $\Delta^2 \hat{X}^Q_{\text{mode}} = 1$ for vacuum state. The maximum achievable variance is given by the maximum eigenvalue of a renormalised covariance matrix

$$\tilde{C} = D^{-1/2} C D^{-1/2},$$

and the optimal mode function reads $D^{-1/2} f_1(t)$, where $f_1(t)$ is the eigenvector of $\tilde{C}$ that corresponds to the largest eigenvalue λ_1 of $\tilde{C}$. The 10 largest eigenvalues of $\tilde{C}$ are plotted in the inset of Fig. S1. We can see that a single eigenvalue clearly stands out, indicating presence of a single well defined mode that can be associated with the two-photon subtracted state.

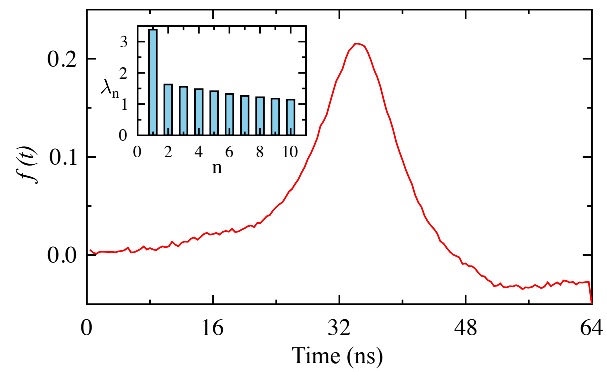

FIG. S1. Optimal temporal mode profile $f(t) \approx f_1(t)$ determined form the measured covariance matrices. The inset shows the 10 largest eigenvalues λ_n of the renormalised covariance matrix $\tilde{C}$ of the signal that contains the two-photon subtracted state.

When performing numerical calculations, we observed that the final multiplication of $f_1(t)$ by $D^{-1/2}$ strongly enhanced the noise at high-frequency components of the mode function while the overall profile of the function almost did not change. We thus found that for our data we could omit the multiplication by $D^{-1/2}$ and use the mode profile $f_1(t)$ as an excellent approximation of the sought optimal mode function $f(t)$. In particular, the maximum eigenvalue of $\tilde{C}$ reads $\lambda_1 = 3.383$, and with the mode profile $f_1(t)$ we got $\Delta^2 X^Q_{mode} = 3.365$, which was very close. For comparison, if we avoided the renormalisation and considered a mode profile f_C corresponding to the largest eigenvalue of the "bare" covariance matrix C, we got $\Delta^2 X^Q_{mode} = 3.220$. The mode function $f_1(t) \approx f(t)$ is plotted in Fig. S1. It was utilised in all subsequent data processing.

We used the same mode function for both balanced homodyne detectors of our 8-port device, just being shifted along the time axis to compensate for slightly different delays. Extra care was taken to design the two detectors such that they provided identical response. Naturally, the temporal dependence of the variance of anti-squeezed quadrature $\hat{X}^Q(t)$ exhibited much better signal-to noise ratio than the squeezed quadrature $\hat{Y}^Q(t)$. Therefore, the $\hat{X}^Q(t)$ data were used to construct the mode function. In fact, in the spectrum of the covariance matrix of the squeezed quadratures $\hat{Y}^Q(t_m)$ it was not possible to identify a single eigenvalue that would unambiguously correspond to the mode in the two-photon-subtracted state. The measured quadratures of the two-photon subtracted state in mode $f_1(t)$ could be determined by integration over the measured 64 ns time window inside which 160 samples were recorded,

$$\hat{X}^Q_{\mathrm{mode}} = \sum_{m=1}^{160} f_+(t_m)\hat{X}^Q(t_m),$$
$$\hat{Y}^Q_{\mathrm{mode}} = \sum_{m=1}^{160} f_+(t_{m-d})\hat{Y}^Q(t_m). \tag{S1}$$

Here $d = 2$ represents the identified offset between temporal delays in the two channels.

QUANTUM STATE TOMOGRAPHY

The 8-port homodyne detector sampled the Husimi Q-function, which represented a tomographically complete measurement. Here, we describe how we extracted the density matrix in Fock basis from the measured 8-port homodyne data. We first constructed a histogram of the measured complex amplitudes β_j. We divided the phase space into rectangular bins with size $d = 1/(8\sqrt{2})$ and centred at $\beta_{mn} = (m+in)d$, where $m, n \in \mathbb{Z}$. We counted the number f_{mn} of measurement outcomes β_j that felt inside the bin (m, n) and we associated a POVM element

$$\Pi_{mn} = \frac{d^2}{\pi}|\beta_{mn}\rangle\langle\beta_{mn}|$$

to each bin.

We represented the operators and density matrices in Fock basis and introduced a cut-off at Fock state $N_{\max} = 21$, which is sufficiently large to accommodate the investigated states with sufficient margin. We reconstructed the density matrix in Fock basis from the measured data f_{mn} using an iterative Maximum-Likelihood reconstruction algorithm [2], that seeks a state that is most likely to yield the observed experimental data. The algorithm naturally imposes all physical constraints on the reconstructed density matrix, namely positive semi-definiteness and unit trace. The likelihood function is defined as

$$\mathcal{L} = \prod_{m,n} (p_{mn})^{f_{mn}}, \tag{S2}$$

where the product is taken over all nonzero f_{mn}, and

$$p_{mn} = \mathrm{Tr}[\hat{\Pi}_{mn}\hat{\rho}] \tag{S3}$$

is the theoretical probability of the measurement outcome $\hat{\Pi}_{mn}$.

It is convenient to work with the log-likelihood function $\ln\mathcal{L}$. The density matrix that maximises $\ln\mathcal{L}$ satisfies the extremal equation [3]

$$\hat{R}\hat{\rho} = \lambda\hat{\rho}, \tag{S4}$$

where

$$\hat{R} = \frac{f_{mn}}{p_{mn}}\hat{\Pi}_{mn}, \tag{S5}$$

and the Lagrange multiplier λ accounts for the constraint $\mathrm{Tr}[\hat{\rho}] = 1$. For a density matrix that maximises $\mathcal{L}$ and satisfies (S4), we get $\lambda = \sum_{m,n} f_{mn}$. Starting from a maximally mixed state in the truncated Fock space the density matrix that maximises $\mathcal{L}$ can be conveniently determined by repeated iterations of the following non-linear map that represents a symmetrised version of the extremal equation (S4) [2],

$$\hat{\rho} \to \frac{\hat{R}\hat{\rho}\hat{R}^\dagger}{\mathrm{Tr}[\hat{R}\hat{\rho}\hat{R}^\dagger]}. \tag{S6}$$

Note that at each iteration step $\hat{R}$ depends on $\hat{\rho}$. This iterative reconstruction algorithm was applied to the original squeezed state, the two-photon subtracted state and a selected distilled state after one round of the gaussification protocol. In all cases a few hundred iterations proved sufficient to reconstruct the state.

The Wigner functions of the states plotted in Fig. 4 of the main manuscript were obtained from the reconstructed density matrices in Fock basis. The reconstructed states were mixed, which could be mainly attributed to the overall losses in the setup and the imperfect two-photon subtraction. It is worth noting that the calculation of a Wigner function from the Husimi Q-functions amounts to a de-convolution, because the Q-function can be expressed as a convolution of the Wigner function with a Gaussian function. From the point of view of the early linear quantum state tomography techniques, this deconvolution, when performed on noisy experimental data, may be difficult to implement and may lead to enhanced noise. However, the non-linear statistically motivated Maximum-Likelihood reconstruction is robust enough to perform reliable quantum state reconstruction of non-classical states of light from the 8-port homodyne data.

GAUSSIFICATION

Here we review the calculation of the covariance matrix of the asymptotic Gaussian state as obtained by iterative Gaussification [4, 5]. Let us first consider the original Gaussification procedure, where at each iteration two copies of the state interfere at a balanced beam splitter and the output port of the beam splitter that corresponds to constructive interference is projected onto vacuum. Upon success the output state at the other port is taken as an input for the next iteration of the protocol. A single step of this Gaussification protocol is described by a nonlinear map

$$\rho^{(j+1)} = \mathrm{Tr}_2\left[\left(\hat{U}_{\mathrm{BS}}\hat{\rho}^{(j)} \otimes \hat{\rho}^{(j)}\hat{U}_{\mathrm{BS}}^{\dagger}\right)\left(\hat{I}_1 \otimes |0\rangle\langle 0|_2\right)\right], \tag{S7}$$

where Tr_2 denotes the trace over the second mode and $\hat{U}_{\mathrm{BS}}$ denotes the unitary matrix of a balanced beam splitter. After the first iteration, the state $\hat{\rho}^{(1)}$ exhibits vanishing coherent displacement, $\langle \hat{X} \rangle = 0$ and $\langle \hat{Y} \rangle = 0$, and also $\rho_{1,0}^{(1)} = 0$ due to destructive interference. If the nonlinear map (S7) converges, the asymptotic state $\hat{\rho}^{(\infty)}$ is Gaussian and its covariance matrix Γ_G can be expressed as [4]

$$\Gamma_G = \Sigma^T B^{-1} \Sigma - I, \tag{S8}$$

where I is the 2×2 identity matrix, Σ denotes the symplectic form,

$$\Sigma = \begin{pmatrix} 0 & 1 \\ -1 & 0 \end{pmatrix},$$

and the matrix B can be expressed in terms of elements of normalised density matrix $\hat{\sigma} = \hat{\rho}^{(1)}/\rho_{0,0}^{(1)}$,

$$B_{11} = \frac{1}{2}\left[1 - \sigma_{1,1} + \sqrt{2}\mathrm{Re}(\sigma_{2,0})\right],$$
$$B_{22} = \frac{1}{2}\left[1 - \sigma_{1,1} - \sqrt{2}\mathrm{Re}(\sigma_{2,0})\right],$$
$$B_{12} = B_{21} = \frac{1}{\sqrt{2}}\mathrm{Im}(\sigma_{2,0}).$$

The protocol will converge to a pure Gaussian state only if $\sigma_{1,1} = 0$, otherwise the asymptotic Gaussian state with covariance matrix (S8) will be mixed.

In our experiment we emulate the Gaussification protocol by processing the complex amplitudes β measured with our 8-port homodyne detector. Consider two experimentally sampled complex amplitudes β_1 and β_2. The complex amplitudes corresponding to destructive- and constructive-interference output ports of the beam splitter read

$$\beta_- = \frac{1}{\sqrt{2}}(\beta_1 - \beta_2), \qquad \beta_+ = \frac{1}{\sqrt{2}}(\beta_1 + \beta_2).$$

The amplitude β_- is accepted as an outcome of a single iteration of the Gaussification protocol if β_+ satisfies suitable acceptance condition. In experimental data processing, we impose a hard boundary $|\beta_+|^2 \leq \bar{n}$. For theoretical analysis, it is more convenient to consider a Gaussian acceptance probability

$$P(\beta) = \exp\left(-\frac{|\beta|^2}{\bar{n}}\right).$$

This acceptance condition gives rise to a modified Gaussification protocol, where one output mode of the beam splitter is effectively projected at the operator

$$\hat{\Pi} = \frac{1}{\pi}\int_\beta P(\beta)|\beta\rangle\langle\beta| d^2\beta = \frac{1}{\pi}\int_\beta \exp\left(-\frac{|\beta|^2}{\bar{n}}\right)|\beta\rangle\langle\beta| d^2\beta, \tag{S9}$$

and the formula (S7) changes to

$$\rho^{(j+1)} = \mathrm{Tr}_2\left[\left(\hat{U}_{\mathrm{BS}}\hat{\rho}^{(j)} \otimes \hat{\rho}^{(j)}\hat{U}_{\mathrm{BS}}^{\dagger}\right)\left(\hat{I}_1 \otimes \hat{\Pi}_2\right)\right], \tag{S10}$$

Up to normalisation, the expression (S11) is the density matrix of a thermal state with mean photon number $\bar{n}$ and we have

$$\hat{\Pi} = \sum_{n=0}^{\infty}\left(\frac{\bar{n}}{\bar{n}+1}\right)^{n+1}|n\rangle\langle n|. \tag{S11}$$

Convergence of generalised Gaussification protocols of the form (S10) was studied by Campbell and Eisert [5], who derived analytical formula for the covariance matrix of the asymptotic Gaussian state for this case. One first defines a non-Hermitian operator

$$\hat{\sigma} = \frac{\hat{\rho}^{(1)}\hat{\Pi}}{\mathrm{Tr}\left[\hat{\rho}^{(1)}\hat{\Pi}\right]}$$

that should exhibit zero coherent displacement, $\mathrm{Tr}[\hat{\sigma}\hat{X}] = \mathrm{Tr}[\hat{\sigma}\hat{Y}] = 0$. Let Γ_σ denote the generally complex-valued covariance matrix of $\hat{\sigma}$ and Γ_Π the covariance matrix of the normalised operator $\hat{\Pi}/\mathrm{Tr}[\hat{\Pi}]$. Note that in the present case we have $\Gamma_\Pi = (1 + 2\bar{n})I$. The covariance matrix of the asymptotic Gaussian state can then be expressed as [5]

$$\Gamma_\infty = (\Gamma_\Pi - i\Sigma)(\Gamma_\Pi - \Gamma_\sigma)^{-1}(\Gamma_\Pi + i\Sigma) - \Gamma_\Pi. \tag{S12}$$

The conditions for a (weak) convergence of the protocol are that the characteristic function of the operator $\hat{\sigma}$ satisfies $|\chi_\sigma(\vec{\xi})| \leq 1$ for all $\vec{\xi}$ and that the covariance matrix Γ_∞ exists and is positive definite.

We now provide an alternative equivalent expression for the covariance matrix Γ_∞ based on the reinterpretation of the Gaussification protocol (S10). Our approach avoids the use of non-Hermitian operators. We observe that a transmission of a quantum state $\hat{\rho}$ through a lossy quantum channel $\mathcal{L}$ with transmittance T followed by projection onto vacuum corresponds to a generalised measurement on the original state $\hat{\rho}$ described by the operator

$$\hat{\Pi}' = \sum_{n=0}^{\infty}(1-T)^n|n\rangle\langle n| = \sum_{n=0}^{\infty}\left(\frac{\bar{n}}{\bar{n}+1}\right)^{n}|n\rangle\langle n|, \tag{S13}$$

where $T = 1/(\bar{n}+1)$. Therefore, $\hat{\Pi}' = \frac{\bar{n}+1}{\bar{n}}\hat{\Pi}$ and the operators (S11) and (S13) are identical up to a multiplicative constant. We next note that interference of two states at a beam splitter followed by transmission of each output state through a lossy channel $\mathcal{L}$ is equivalent to transmission of each input state through a lossy channel followed by interference at a beam splitter. Consequently, we can consider a modified input state $\hat{\rho}^{(1)}_{\mathcal{L}} = \mathcal{L}(\hat{\rho}^{(1)})$ and determine from Eq. (S8) the covariance matrix Γ_G for the original Gaussification protocol with projection onto vacuum. This covariance matrix must be interpreted as a covariance matrix of the asymptotic state transmitted through the lossy channel, $\Gamma_G = T\Gamma_\infty + (1-T)I$. This relation can be inverted and we get

$$\Gamma_\infty = \frac{1}{T}\left[\Gamma_G - (1-T)I\right]. \tag{S14}$$

Numerical calculations confirm that the formulas (S12) and (S14) yield the same covariance matrices. We take the reconstructed density matrix of the two-photon subtracted squeezed vacuum state and calculate the covariance matrix Γ_∞ of the asymptotic state of the Gaussification protocol for various thresholds $\bar{n}$. We find that for our state the Gaussification protocol converges for $\bar{n} > 0.3$. The distilled Gaussian state is mixed and close to this threshold the variance of the anti-squeezed quadrature becomes arbitrarily large, while the amount of distillable squeezing becomes limited, $\Delta^2 Y \gtrsim 0.35$. Therefore, it is reasonable to choose larger acceptance threshold $\bar{n}$ as it also increases the success rate of the protocol, c.f. Fig. 5 in the main text.

PHOTON SUBTRACTION AUGMENTED BY COHERENT DISPLACEMENT

Here we discuss a more general photon subtraction operation, which is combined with a coherent displacement operation resulting in the conditional operation $\hat{a} + \delta$. This operation can be implemented either by coherently displacing the signal before or after the photon subtraction,

$$\hat{D}(-\delta)\hat{a}\hat{D}(\delta) = \hat{a} + \delta, \tag{S15}$$

or, more conveniently, by coherently displacing the tapped mode that is detected by the single photon detector [6]. Here we consider a combination of two such 'displaced photon subtractions' and choose the two coherent amplitudes such that the resulting operation preserves the parity of Fock states,

$$\hat{M} = (\hat{a}+\delta)(\hat{a}-\delta) = \hat{a}^2 - \delta^2. \tag{S16}$$

Since δ is a complex amplitude, δ^2 can be negative as well as positive. Application of the generalised two-photon subtraction (S16) to pure squeezed vacuum state $|\psi(r)\rangle$ yields the non-normalised state

$$|\psi_{2S}(r)\rangle = \frac{1}{\sqrt{\cosh(r)}}\sum_{n=0}^{\infty}\left[(2n+1)\tanh r - \delta^2\right](\tanh r)^n \frac{\sqrt{(2n)!}}{2^n n!}|2n\rangle. \tag{S17}$$

The variances of the amplitude and phase quadratures of this state can be expressed as

$$\begin{aligned}\Delta^2\hat{X} &= e^{2r}\left[1 + 4\sinh^2 r\frac{2\sinh^2 r + \cosh r\sinh r - \delta^2}{2\sinh^4 r + (\cosh r \sinh r - \delta^2)^2}\right],\\ \Delta^2\hat{Y} &= e^{-2r}\left[1 + 4\sinh^2 r\frac{2\sinh^2 r - \cosh r\sinh r + \delta^2}{2\sinh^4 r + (\cosh r \sinh r - \delta^2)^2}\right].\end{aligned} \tag{S18}$$

The amplitude δ can be chosen to minimise the squeezed variance of the two-photon subtracted state. Minimisation of $\Delta^2\hat{Y}$ with respect to δ^2 yields

$$\delta^2 = \cosh r\sinh r - (2+\sqrt{6})\sinh^2 r.$$

For this amplitude, the quadrature variances of the two-photon subtracted state (S17) become

$$\Delta^2\hat{X} = \frac{7+2\sqrt{6}}{3+\sqrt{6}}e^{2r}, \qquad \Delta^2\hat{Y} = \frac{3}{3+\sqrt{6}}e^{-2r},$$

hence the optimised photon subtraction increases the squeezing by 2.6 dB for arbitrary initial squeeze parameter r. This procedure can generate a state with finite squeezing from arbitrarily weakly squeezed input state, but the success probability of photon subtraction will decrease with decreasing r and will scale as $\sinh^4 r$.

The squeezing of the photon subtracted state can be further increased by iterative Gaussification. The final squeeze parameter of the gaussified state r_{G} can be expressed as

$$\tanh r_{\mathrm{G}} = \frac{3\tanh r - \delta^2}{\tanh r - \delta^2}\tanh r.$$

This expression is meaningful and the gaussification converges only if $|\tanh r_{\mathrm{G}}| < 1$. Note that any required squeezing $s > r$ is in principle achievable for any nonzero input squeezing r, if we set

$$\delta^2 = \frac{\tanh r_{\mathrm{G}} - 3\tanh r}{\tanh r_{\mathrm{G}} - \tanh r} \tanh r.$$

Therefore, arbitrary strong squeezing can be distilled from arbitrary weak initial squeezing by combination of the displacement-enhanced two-photon subtraction (S16) followed by iterative Gaussification.

* roman.schnabel@physnet.uni-hamburg.de

[1] Morin, O., Fabre, C. & Laurat, J. Experimentally Accessing the Optimal Temporal Mode of Traveling Quantum Light States. *Physical Review Letters* **111**, 213602 (2013). URL http://link.aps.org/doi/10.1103/PhysRevLett.111.213602. arXiv:1307.6364v1.

[2] Ježek, M., Fiurášek, J. & Hradil, Z. Quantum inference of states and processes. *Physical Review A* **68**, 012305 (2003). URL https://link.aps.org/doi/10.1103/PhysRevA.68.012305. 0210146.

[3] Hradil, Z. Quantum-state estimation. *Physical Review A* **55**, R1561–R1564 (1997). URL https://link.aps.org/doi/10.1103/PhysRevA.55.R1561. 9609012.

[4] Eisert, J., Browne, D., Scheel, S. & Plenio, M. Distillation of continuous-variable entanglement with optical means. *Annals of Physics* **311**, 431–458 (2004). URL https://linkinghub.elsevier.com/retrieve/pii/S0003491604000041. 0307106.

[5] Campbell, E. T. & Eisert, J. Gaussification and Entanglement Distillation of Continuous-Variable Systems: A Unifying Picture. *Physical Review Letters* **108**, 020501 (2012). URL https://link.aps.org/doi/10.1103/PhysRevLett.108.020501.

[6] Neergaard-Nielsen, J. S. *et al.* Optical Continuous-Variable Qubit. *Physical Review Letters* **105**, 053602 (2010). URL https://link.aps.org/doi/10.1103/PhysRevLett.105.053602. 1002.3211.